

# Space-variant optical correlator based on the fractional Fourier transform: implementation by the use of a photorefractive $\text{Bi}_{12}\text{GeO}_2$ (BGO) holographic filter.

Sergio Granieri, María del Carmen Lasprilla, Néstor Bolognini, and Enrique E. Sicre

A space-variant optical correlator is proposed on the basis of the fractional Fourier transform. The optical device uses as a recording medium for the holographic filter a photorefractive  $\text{Bi}_{12}\text{GeO}_2$  (BGO) crystal. The experimental results confirm the shift-variance properties. Some limitations that arise from the volume diffraction are also considered. © 1996 Optical Society of America

The basic VanderLugt optical correlator detects the similarity between a certain input object and a reference object that is stored as pure spectral information in a holographic filter.<sup>1</sup> In this way, the recognition device results are space invariant, i.e., the correlation output simply translates as the input object moves, leaving the correlation peak unchanged. Shift invariance is in general useful for target-localization purposes, but it can be a drawback in some applications in which both the localization of the object and its identity become relevant for positioning requirements. Thus, some methods were developed for obtaining space-variant holographic filters that employ reference beams having different angles<sup>2</sup> or phase encoding.<sup>3</sup>

More recently, Davis *et al.*<sup>4</sup> introduced a Fresnel-transform correlator in which the Fresnel pattern diffracted by the input transparency in free-space propagation interacts with the filter mask. The Fresnel-transform operation gives rise to spatially dependent phase shifts to the input object, thus creating the space-variance properties. Related to this technique, a generalized VanderLugt filtering approach was proposed in which the ordinary optical

Fourier transform involved in the spectral definition of the conventional correlation is replaced by fractional Fourier transforms (FFR's).<sup>5-7</sup> The fractional correlation so obtained stores information about the input object both in a spectral and a space domain, something that can be expected because the fractional correlation can be expressed as phase-space slices of a Wigner-distribution function.<sup>5</sup>

In this Note we propose an optical implementation of the fractional correlation by using a photorefractive  $\text{Bi}_{12}\text{GeO}_2$  (BGO) crystal as a real-time recording medium of the holographic filter. The optical configuration is schematized in Fig. 1. The photorefractive-material plate  $H$  stores the interference pattern between the reference beam and the FFR of the object  $O$ . This operation is achieved by means of the lens  $L_1$ , as it was analyzed in Ref. 8. In this way, the recorded intensity distribution can be written as

$$I_H(x) = |U^{(r)}(x; \theta) + F^{(p)}\{t(x_0)\}|^2 = \left| U^{(r)}(x; \theta) + \exp\left(\frac{i\pi x^2}{\lambda f_0 \tan \phi}\right) \int_{-\infty}^{\infty} t(x_0) \times \exp\left(\frac{i\pi x_0^2}{\lambda f_0 \tan \phi}\right) \exp\left(\frac{-i2\pi x x_0}{\lambda f_0 \sin \phi}\right) dx_0 \right|^a, \quad (1)$$

where  $U^{(r)}(x; \theta)$  is the amplitude of the reference beam and, for simplicity, a one-dimensional object transparency  $t(x_0)$  was assumed. The order  $p$  ( $0 \leq p \leq 1$ ) of the FFR  $F^{(p)}\{t(x_0)\}$  can be selected according to the relation:  $z_0 = f_0 \tan(\phi/2)$  and  $\phi = p\pi/2$ . For

The authors are with the Centro de Investigaciones Ópticas (CIO<sub>p</sub>), C.C. 124, 1900 La Plata, Argentina. S. Granieri and N. Bolognini are also with the Facultad de Ciencias Exactas, Universidad de La Plata, Argentina; and M. del Carmen Lasprilla is with the Universidad de Santander, Bucaramanga, Colombia.

Received 24 January 1996; revised manuscript received 2 August 1996.

0003-6935/96/356951-04\$10.00/0

© 1996 Optical Society of America

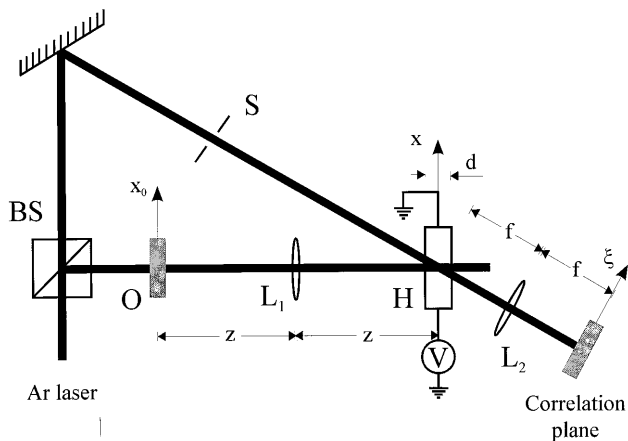


Fig. 1. Experimental setup.

$p = 1$ , Eq. (1) reduces to the well-known VanderLugt holographic filter.

In a second step, the shutter  $S$  cancels the reference beam in such a way that the photorefractive filter  $H$  is illuminated only by  $U_p(x) = F^{(p)}\{t(x_0)\}$ . A second lens  $L_2$ , having a focal length  $f$ , performs the ordinary ( $p = 1$ ) Fourier transform of one of the four terms of the amplitude transmitted by  $H$  [which is proportional to the expression given by Eq. (1)]. Thus, at the back focal plane of  $L_2$ , the fractional correlation output is obtained as

$$I(\xi) = |F^{(1)}[F^{(p)}\{t(x_0)\}F^{(p)*}\{t(x_0)\}]_{(\xi/\lambda f)}|^2. \quad (2)$$

Some properties of Eq. (2) related with space-variant pattern recognition were analyzed and experimentally verified in Refs. 6 and 7.

Photorefractive crystals have been widely used in image processing.<sup>9</sup> These materials are well suited for real-time recording because of their ability to store light intensity distributions as a refractive-index pattern without chemical-development procedures. The sillenite type crystals like BGO combine a high sensibility and fast response with their inherent reversibility.<sup>10,11</sup> Hence, they are particularly well suited as dynamic volume holographic media for matched-filtering correlation. Of course, after the information is stored, it can be retrieved for pattern-recognition purposes or other optical-processing operations.

As a light source an expanded and collimated argon-ion laser beam with a wavelength of  $\lambda = 514.5$  nm was used from which the beam splitter (BS) produces two coherent beams. One of the beams illuminates the input transparency  $O$ , and the lens  $L_1$  generates the FFR on the photorefractive BGO crystal, while the other beam acts as a reference. Both beams interfere in the crystal volume being the average external angle between them:  $\theta \cong 7.4^\circ$ . In this way the filter was synthesized. During the correlation operation the reference beam was blocked out by the shutter  $S$ , so the input pattern became a reference image or reading beam illuminated by the same wavelength.

For improving the diffraction efficiency, a voltage of  $V = 8$  kV was applied between the  $[110]$  faces, which are separated a distance of  $t = 10$  mm, producing an electric field of  $E_a = 0.8$  kV/mm. The directions  $\langle 1\bar{1}0 \rangle$ ,  $\langle 001 \rangle$ , and  $\langle 110 \rangle$  coincide with the crystal edges. The crystal thickness  $d$  was set along the  $\langle 110 \rangle$  direction. An effective intensity of  $20$  mW/cm<sup>2</sup> was utilized in the write-in process. For synthesizing the filter an input transparency with a letter S character  $2$  mm high and  $1.5$  mm wide was utilized. The focal length of lens  $L_1$  was  $f_0 = 570$  mm. The interference fringes created by the superposition of the FFR and reference beam were recorded over a period of  $3$  min. Then, the holographic filter was sequentially read out by the reference image. During the read-out process an effective intensity of  $20$  mW/cm<sup>2</sup> was employed, and the input pattern  $O$  was translated to a fixed length between successive readings (of  $1$  s each). A CCD camera was used to acquire the experimental data, which were transmitted to a computer, digitalized, and stored in a frame grabber. Besides, the computer commanded each translation step in the displacement of the reference image. The acquisition system discriminates  $256$  intensity levels.

To demonstrate the shift-variance nature of the FFR we took some measurements of the correlation-peak intensity in terms of the in-plane displacements of the reference image. Nevertheless, it should be noted that a photorefractive-based correlator experiences Bragg diffraction limitations because of the finite crystal thickness  $d$ . In other words, if the reading beam is not matched with the writing beam a corresponding dephasing wave vector appears, which reduces the diffraction efficiency. Hence, in our case, this effect will contribute to a decrease in the correlation-peak intensity above that which the shift-variance nature of the correlator would produce in any case.

In Figs. 2 and 3 are shown the experimental values of the normalized correlation-peak intensity in terms of different displacements. Figures 2(a) and 3(a) and Figs. 2(b) and 3(b) correspond to cases of different crystal thicknesses:  $d = 1$  mm and  $d = 3$  mm, respectively. Also, three fractional orders  $p$  are implemented in each graphic.

Let us consider Fig. 2. In the read-out process the reference image has been displaced in  $x_0$  direction. Because of the shift-invariance property, the experimental points for  $p = 1$  should maintain constant values. Nevertheless a decrease in the correlation values is observed in accordance with the Bragg mismatch introduced by the displacement. This behavior indicates that, when a specific grating component is Bragg matched, the diffraction efficiency reaches the maximum. As far as the shift is introduced, the amplitude diffraction coefficient decreases as a sinc function with respect to the mismatch.<sup>11</sup> The width of the sinc function is proportional to the square of the employed focal length and inversely proportional to both the shift and the crystal thickness.<sup>10</sup> In the case shown in Fig. 2(b) ( $d = 3$  mm) for  $p = 1$  a reduced shift tolerance is clearly shown in comparison with

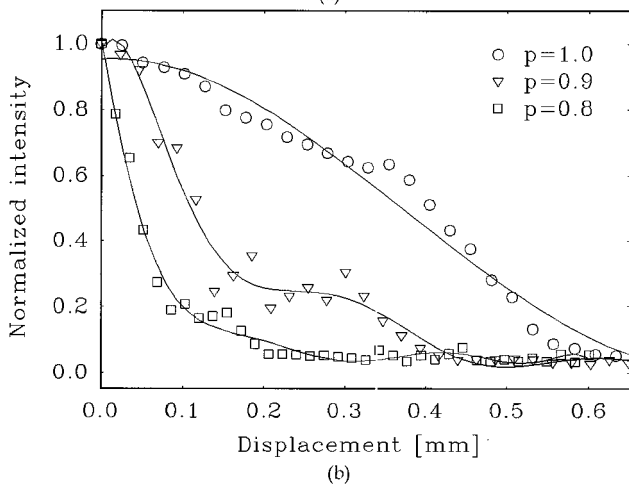
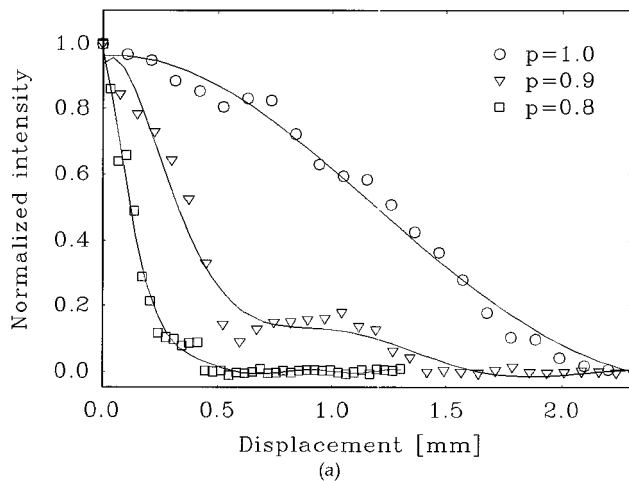


Fig. 2. Correlation-peak intensity versus the object lateral displacement: (a) for a thickness of  $d = 1$  mm and (b) for a thickness of  $d = 3$  mm.

the case from Fig. 2(a) ( $d = 1$  mm) for a given level in the correlation intensity. Besides, it is clear that, for  $p = 0.9$  and  $p = 0.8$ , a stronger intensity decrease is observed. In these cases, an additional mismatch is introduced in comparison with  $p = 1$  because of the inherent shift variance that the FFR produces. Notice that in Fig. 2 the curves corresponding to the same values of  $p$  have the same behavior; however, they have a different scale factor because of the change in the crystal thickness [see the displacement range in both cases, Figs. 2(a) and 2(b)].

In Fig. 3 the normalized correlation intensity is shown for the case in which the reference is perpendicularly translated to the  $x_0$ - $z$  plane. Such displacements should not introduce Bragg mismatch because the index gratings stored in the filter have their grating vectors perpendicular to these displacements. The diffracted intensity is practically insensitive to the volume effect of the recording medium, and the situation can be compared with that of a plane hologram. To prove this assertion Fig. 4 displays the computed fractional correlation for different orders of a plane holographic

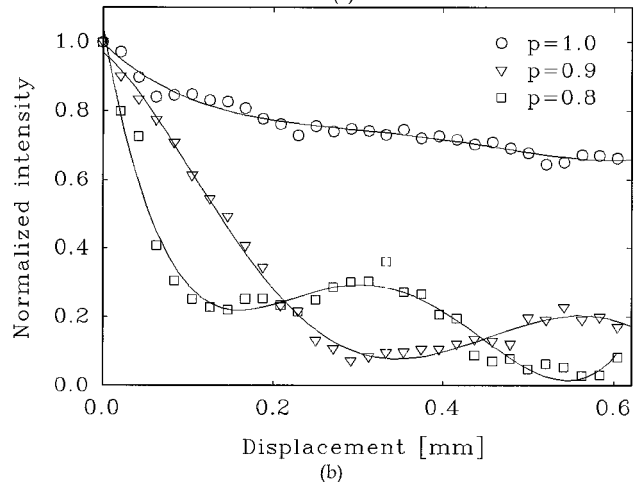
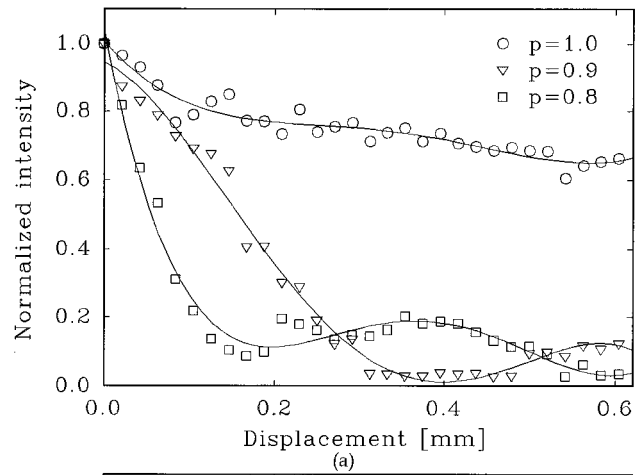


Fig. 3. Correlation-peak intensity versus the object displacement perpendicular to the  $x_0$ - $z$  plane: (a) for a thickness of  $d = 1$  mm and (b) for a thickness of  $d = 3$  mm.

filter ( $d = 0$ ). There, the well-known shift-invariant behavior for  $p = 1$  is observed. Besides, when  $p < 1$ , a fall-off of the correlation-peak value with increasing shift appears. That is, in cases of  $p < 1$ , the correlations peaks experience a clear shift-variant behavior.

Returning now to the experimental data shown in Fig. 3, it can be observed that the fitted curves for  $p < 1$  in Figs. 3(a) and 3(b) are similar to the corresponding computed curves of Fig. 4. That is, only the experimental values belonging to the order  $p = 1$  exhibit shift-invariant behavior. Notice that, because of the dynamic nature of the crystal, the stored information slowly disappears as a result of charge diffusion, and the read-out process also decreases the relaxation time. These effects contribute to the slight decrease of the peak value for  $p = 1$  that the experimental data exhibit; otherwise the intensity would remain constant. A routine that involves periodic refreshing of the filter would correct these drawbacks. In cases of  $p = 0.9$  and  $p = 0.8$ , the correlation peaks show clear shift-variant behavior. It should also be emphasized that the distribution of the experimental data does not depend on the crystal

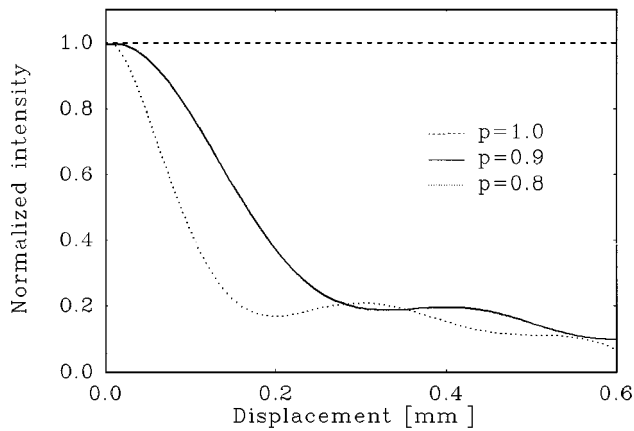


Fig. 4. Correlation-peak intensity versus the object displacement perpendicular to the  $x_0$ - $z$  plane: computed curves for a plane holographic filter.

thickness but on the fractional order, as is clearly observed from Fig. 3.

A real-time correlator based on the FFR has been implemented. The proposed approach, based on fractional correlation, has the advantage over other space-variant techniques in that its sensitivity to detect object displacement can be adjusted simply by modification of the relative positions among the object, the lens, and the filter of the optical system. A thick photorefractive crystal served as the dynamic material for recording the holographic filter as a spatial perturbation of the refractive index. Because of the high crystal storing capacity, a set of such filters could be recorded in the volume medium, each one associated with a different input, for instance, in an angle-multiplexing schedule.<sup>12</sup> In this case, each input could represent a certain order of the FFR, so that a set of matched filters could be stored for a given input and different  $p$  orders. On the other hand, the limitations that are inherent to volume diffraction

can be reduced by the employment of the well-known techniques for conventional correlators.<sup>13</sup>

This work was supported by the Consejo Nacional de Investigaciones Científicas y Técnicas (CONICET), Argentina.

## References

1. A. VanderLugt, "Signal detection by complex spatial filtering," *IEEE Trans. Inf. Theory* **IT-10**, 139–145 (1964).
2. L. M. Deen, J. F. Walkup, and M. O. Hagler, "Representations of space-variant optical systems using volume holograms," *Appl. Opt.* **14**, 2438–2446 (1975).
3. T. F. Krile, R. J. Marks, J. F. Walkup, and M. O. Hagler, "Holographic representations of space-variant systems using phase-coded reference beams," *Appl. Opt.* **16**, 3131–3135 (1977).
4. J. A. Davis, D. M. Cottrell, N. Nestorovic, and S. M. Highnote, "Space-variant Fresnel transform optical correlator," *Appl. Opt.* **31**, 6889–6893 (1992).
5. S.-Y. Lee and H. H. Szu, "Fractional Fourier transform, wavelet transform, and adaptive neural networks," *Opt. Eng.* **33**, 2326–2330 (1994).
6. D. Mendlovic, H. M. Ozaktas, and A. W. Lohmann, "Fractional correlation," *Appl. Opt.* **34**, 303–309 (1995).
7. D. Mendlovic, Y. Bitran, R. G. Dorsch, and A. W. Lohmann, "Optical fractional correlation: experimental results," *J. Opt. Soc. Am. A* **12**, 1665–1670 (1995).
8. A. W. Lohmann, "Image rotation, Wigner rotation, and the fractional Fourier transform," *J. Opt. Soc. Am. A* **10**, 2181–2186 (1993).
9. P. Günter and J. P. Huignard, eds., *Photorefractive Materials and their Applications II*, (Springer-Verlag, Berlin, 1989), pp. 205–271.
10. F. T. S. Yu and S. Yin, "Bragg diffraction-limited photorefractive crystal-based correlators," *Opt. Eng.* **34**, 2224–2231 (1995).
11. C. Gu, H. Fu, and J.-R. Lien, "Correlation patterns and cross-talk noise in volume holographic optical correlators," *J. Opt. Soc. Am. A* **12**, 861–868 (1995).
12. J. V. Alvarez Bravo, N. Bolognini, and L. Airzmendi, "Cross-talk in multiplexed holograms using angular selectivity in  $\text{LiNbO}_3$ ," *Opt. Mater.* **4**, 414–418 (1995).
13. C. Gu, J. Hong and S. Campbell, "2-D shift-invariant volume holographic correlator," *Opt. Commun.* **88**, 309–314 (1992).